FERMI LINAC UPGRADE: COMMISSIONING EXPERIENCE OF THE FIRST S-BAND HIGH-GRADIENT MODULE

N. Shafqat*, F. Gelmetti, C. Maschiovecchio, M. Milloch, A. Milocco, M. Trovo
Elettra Sincrotrone Trieste S.C.p.A., Trieste, Italy

Abstract

The FERMI seeded free-electron laser (FEL), located at the Elettra laboratory in Trieste, is a 4th-generation light source operating in the vacuum ultraviolet to soft X-rays range. In order to extend the FEL spectral range to shorter wavelengths, an increase in the linear accelerator (linac) energy from 1.5 to 2.0 GeV is required. S-band HG module is designed to fulfill the upgrade requirement of 30 MV/m accelerating gradient with the breakdown rate (BDR) in the range of low 10^{-8} bpp/m. One HG module consists of two HG structures, 3.0 m in length, and one Spherical Pulse Compressor (SPC). The 1st HG module is successfully commissioned at the FERMI linac up to an accelerating gradient of 27 MV/m with the BDR of around 5×10^{-8} bpp/m. In this paper, we share the commissioning experience of the HG module from installation, conditioning, high power operation, and commissioning with the beam.

INTRODUCTION

FERMI FEL, located at Elettra Sincrotrone, Trieste, Italy, is a 4th-generation light source operating in Extreme-Ultraviolet (EUV) to soft X-rays. FERMI is driven by a 1.5 GeV normal-conducting S-band linac outlined in Fig. 1. An upgrade plan to reach the shorter wavelength of 4 nm to cover the whole water window is underway [1]. One component of this upgrade plan aims to increase the linac energy from the present 1.5 GeV to 2.0 GeV and improve the beam quality. This goal will be achieved by replacing the existing Backward Traveling Wave (BTW) accelerating structures and SLEDs pulse compressors with the newly designed HG accelerating structures and spherical pulse compressors, as shown in Fig. 2.

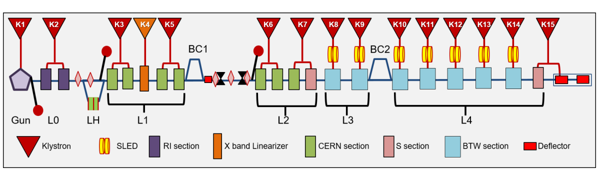

Figure 1: The layout of the existing FERMI linac.

COMMISSIONING OF HG MODULE

HG modules are designed to fulfill the FERMI requirement of 30 MV/m accelerating gradient with the breakdown rate (BDR) in the range of low 10^{-8} bpp/m [**?**]. One HG module consists of two HG accelerating structures, each 3.0 m long, and one SPC. RF parameters of the HG structures are listed in Table 1.

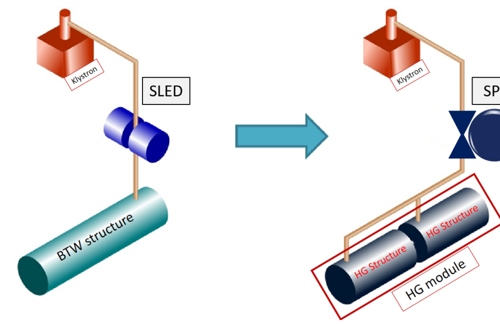

Figure 2: FERMI linac upgrade plan to replace BTWs and SLEDs with the HG modules and SPC.

Table 1: RF Parameters of the HG Structure

Parameter	Value	Unit
f_0	2998.01	MHz
Mode	$2\pi/3$	–
$L_{prototype}$	353.332	mm
L_{cell}	33.332	mm
N_{cell}	84	–
$N_{coupler}$	2	–
Iris radius a	11.382–8.801	mm
Cell radius b	41.610–41.076	mm
R_{shunt}	72–81	MΩ/m
Q_0	≈ 15850	–
v_g/c	2.07–0.97	–
t_f	≈ 645	ns
τ	0.385	Neper

Installation of HG Module

After successful testing and conditioning of the first HG structure (HG1) at the Elettra high-power test facility, the 2nd HG structure (HG2) was directly installed in the FERMI linac at K15 in place of one accelerating section and one deflector, as shown in the Figures. 3 and 4. The goal was to condition the HG2 structure on the FERMI linac in the available time slots between the user beam operation. The HG module was installed with the Barrel Open Cavity (BOC) type pulse compressor due to the delay in the delivery of SPC.

Conditioning of HG Module

The first problem encountered at the start of conditioning was the bad vacuum in the re-combiner region. As shown in Fig. 5, a re-combiner is installed at the output of a two-armed klystron used to feed the HG module, 4th port of which is terminated with a small ferrite-based RF terminator. Initially, the bad vacuum in this region was attributed to degassing but when it persisted, and further investigations were performed,

* nuaman.shafqat@elettra.eu

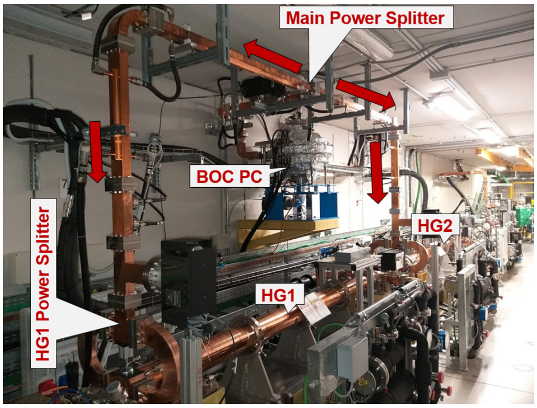

Figure 3: HG1 structure installed in the FERMI linac tunnel.

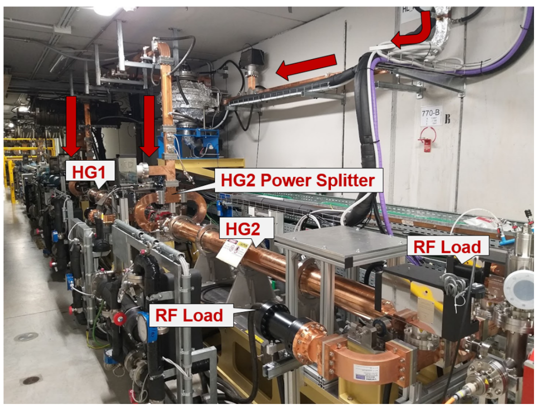

Figure 4: HG2 structure installed in the FERMI linac tunnel.

it was found that the ferrite in the terminator was cracked, resulting in bad vacuum and slowing the conditioning process. The RF terminator was finally replaced with the RF water load as shown in Fig. 5, solving the issue of bad vacuum.

The second issue was related to the vacuum peaks originating from the output side of both HG structures, causing frequent vacuum interlocks. The system was reopened to investigate the issue and revealed the arcing signs on two out of four commercial water loads, as shown in Fig. 6. In order to be prudent, all four RF water loads were replaced with the already tested RF water loads, allowing the conditioning to proceed.

The third problem was related to the frequent arcing, triggering the reflected power interlock defined at the output of the klystron. These events were accompanied with the huge vacuum spikes. BOC was moved from the test facility where it operated to the peak powers of 125 MW, but these arcs were happening as low as 20 MW power from BOC. Further complicating the issue was the fact that such arcs mostly occur in series where one fault triggered sometimes seven faults in a row, forcing the reduction of power level in the system and starting conditioning again. As shown in Fig. 7, two mitered bends were installed after BOC. Eventually, these bends were replaced with already conditioned bends.

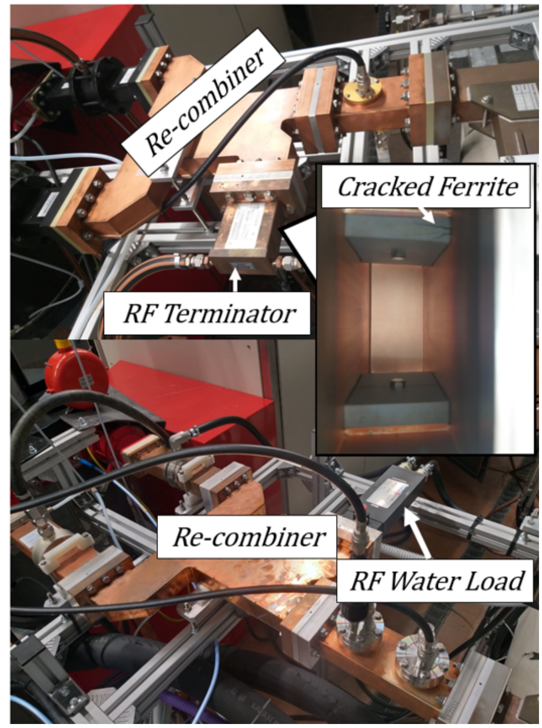

Figure 5: The cracked ferrite terminator at the re-combiner replaced with the RF water load.

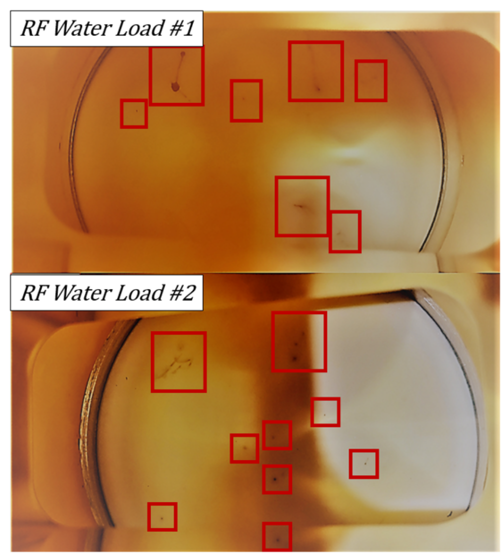

Figure 6: The RF windows of the replaced commercial water loads showing signs of arcing, circled in red.

REACHING 27 MV/M

After two years of rigorous conditioning, we were able to push full power from 45 MW, 4.5 μs klystron to HG module. The energy gain was measured with the electron beam translating to an accelerating gradient of 27 MV/m, a bit shy of the target 30 MV/m. Figure 8 shows the RF pulses at full power.

Constant Power Operation

During 2025, K15 was put online for user beam operation at full power from klystron. Figure 9, shows the vacuum

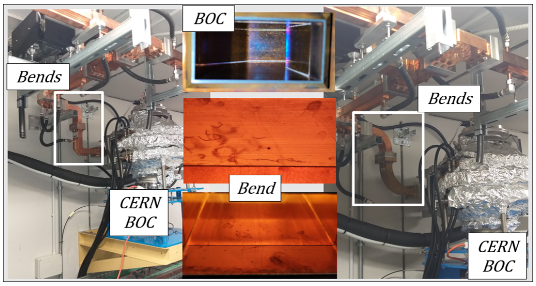

Figure 7: The replacement of the bends after BOC due to arcing issue.

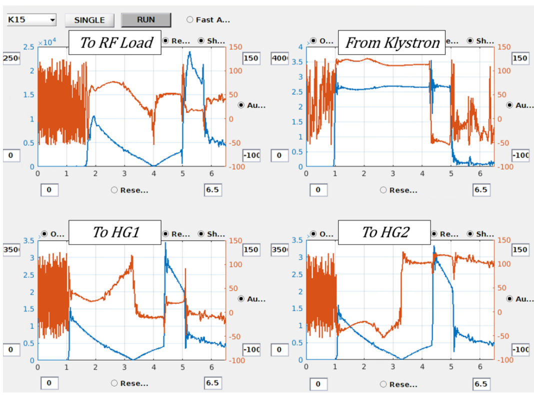

Figure 8: The RF pulses at K15, blue is the amplitude and red is the phase.

trends in the waveguide system and two HG structures, while Fig. 10 shows the fault trend during one sample period. In Fig. 10, the kly faults are the faults due to the arcing at the klystron while RFLA faults represent the arcing taking place in HG module and the feeding system.

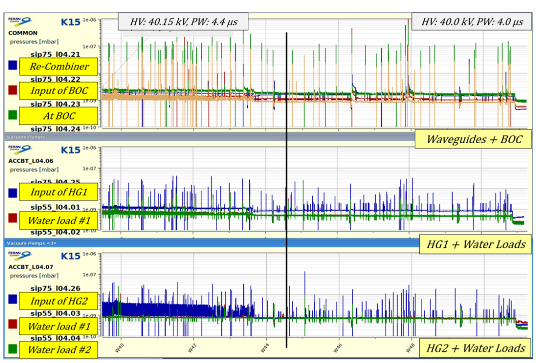

Figure 9: The real vacuum trend during the constant power operation during the winter run.

Analysis of Faults

More than 90 percent of faults are coming from the BOC region and sometimes occur in series, one example of which is shown in Fig. 11. After the replacement of bends, these faults are now attributed to BOC itself. The second type of faults are those coming from the input of HG1 accompanied by very small vacuum peaks. Though occurs rarely, but they sometimes trigger series of faults, an example of which is shown in Fig. 12.

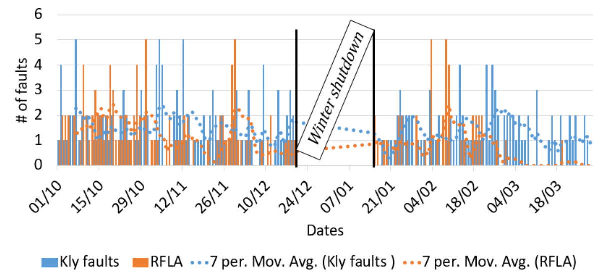

Figure 10: Fault trend for the HG module for 21 weeks of operation with the beam.

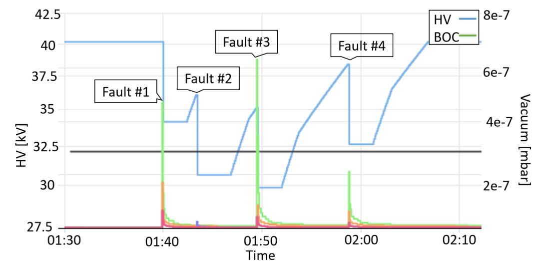

Figure 11: Example of the long fault in the BOC region.

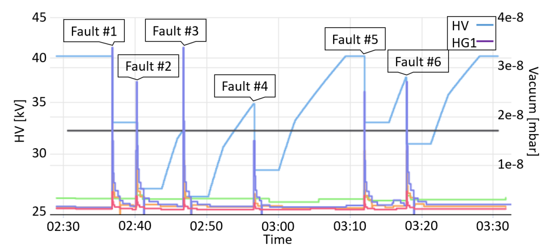

Figure 12: Example of long fault at the HG1.

CONCLUSION

The first S-band HG module is successfully installed and commissioned at the FERMI linac achieving a stable operation at an accelerating gradient of 27 MV/m. The target 30 MV/m was not achieved due to the limited power available from the klystron BOC compressor system. While HG structures worked seamlessly, issues were faced from the waveguide system, slowing the conditioning process and replacements. Faults from BOC region, though improved significantly still persist and contribute more than 90 percent to the downtime from HG module.

REFERENCES

[1] L. Gianessi *et al.*, "FERMI 2.0 Conceptual Design Report," Elettra Sincrotrone Trieste, 2022. https://www.elettra.eu/lightsources/fermi/fermi-machine/fermicdr.html

[2] N. Shafqat *et al.*, "Fabrication, conditioning and installation of the 1st high gradient S-band accelerating module for the energy upgrade of the FERMI free electron laser linac", *Nucl. Instrum. Methods Phys. Res. A*,vol. 1055, p. 168543, 2023. doi:10.1016/j.nima.2023.168543